CONTROLO 2008
8th Portuguese Conference on Automatic Control
University of Trás-os-Montes and Alto Douro, Vila Real, Portugal
July 21-23, 2008

UNDERWATER VEHICLE TRACKING SYSTEMS: MOTION MODELS AND PERFORMANCE ANALYSIS[1]

Pedro M. S. Valverde, Paulo Oliveira, Carlos Silvestre
{pvalverde, pjcro, cjs}@isr.ist.utl.pt
Instituto Superior Técnico (IST), Institute for Systems and Robotics (ISR), Lisbon, Portugal

Abstract: This paper addresses the problem of nonlinear tracking filter design, to estimate the position and attitude of underwater vehicles from range and bearing measurements. Two different nonlinear kinematic models of the vehicle are presented and the behaviour of the respective tracking filters evaluated for different measurement noise levels. Bounds on the attainable performance for the nonlinear estimation problem are presented using the Cramér-Rao Lower Bound and the Posterior Cramér-Rao Lower Bound, in static and dynamic scenarios, respectively. The proposed trackers are validated using measurements provided by a range and bearing sensor under realistic operation conditions, resorting to a set of Monte Carlo simulations. Their performance is then compared to the respective bounds.

Keywords: Marine vehicles; Navigation and Tracking systems; Extended Kalman filters; Vehicle dynamics;

1. INTRODUCTION

During the last decade the number of operational Autonomous Underwater Vehicles (AUVs) and Remotely Operated Vehicles (ROVs) experienced a large increase in interest. The missions to be carried out by the underwater vehicles became also more complex and it is now common their use in environmental monitoring, geological and biological surveys, and underwater structures inspection (e.g. harbours and pipelines). To improve the success of those missions and for security purposes, the position of the underwater vehicle is important to be known at surface, e.g. by a support vessel. The solution to this problem can be casted in the design of a target tracker (Alcocer et al, 2007). Interestingly, methodologies for the design of underwater trackers can profit from the mature field of knowledge in similar aerospace applications, see (Rong and Jilkov, 2003) and the references therein.

The structure of the paper is the following: in section 2 the Extended Kalman Filter (EKF) will be introduced and its structure outlined. The range and bearing sensor that will be used to provide measurements of the underwater target will be briefly discussed in section 3. In section 4, two dynamic models for tracking purposes in two dimensions are proposed: a circular motion dynamic model and a constant turn model with known turn rate. Next, for each model an Extended Kalman Filter (EKF) is implemented to estimate the position of the target and the results obtained from a series of Monte Carlo simulation tests with representative trajectories will be summarized. Tools for the comparative study of nonlinear estimation solutions are introduced in section 5. The performance of the designed EKFs Lower Bound and the Posterior Cramér-Rao Lower Bound, for the static and dynamic scenarios, for both nonlinear models are compared with the lower bounds just introduced, in section 6, and finally some conclusions are drawn in section 7.

[1]This work was partially supported by Fundação para a Ciência e a Tecnologia (ISR/IST plurianual funding) through the POS Conhecimento Program that includes FEDER funds and by the project PDCT/MAR/55609/2004 - RUMOS of the FCT.

2. DISCRETE-TIME KALMAN FILTER

The Kalman filter (KF) is the optimal estimator for linear systems disturbed by Gaussian noise, providing state estimates with least square error (Brown and Hwang, 1997) (Gelb, 1974). In the case of nonlinear dynamic systems or in the presence of nonlinear sensor measurements of the system state, as is the case of range and bearing based tracking filters, other techniques must be thought. The most commonly used is the Extended Kalman Filter (EKF), a sub-optimal estimation method that generalises the KF for nonlinear systems, detailed next.

Consider a nonlinear dynamic system described by

$$\begin{cases} \mathbf{x}_{k+1} = \phi\left(\mathbf{x}_k, k\right) + \mathbf{w}_k \\ \mathbf{z}_k = h\left(\mathbf{x}_k, k\right) + \mathbf{v}_k \end{cases} \tag{1}$$

where $\mathbf{x_k} \in R^n$ is the system state at time k represented as a column vector, ϕ: $R^n \rightarrow R^n$ is the nonlinear time-varying function that describes the state dynamics, h: $R^n \rightarrow R^n$ relates the available sensors measurements $\mathbf{z_k} \in R^m$

with the system state. The measurements are assumed to be disturbed by zero mean Gaussian white-noise $\mathbf{w_k} \in R^n$, and the system dynamics are also considered to be disturbed by zero mean Gaussian white-noise $\mathbf{v_k} \in R^m$.

The EKF attempts to minimize the pseudo-covariance of the estimation error resorting to a recursive structure composed by two steps: the prediction step – where the state mean and the pseudo-covariance are computed given the system dynamics; and the update step – where the predicted state is corrected using the information available from the sensor measurements. The equations for each one of these steps are described below.

Prediction step: In this step the predicted error state pseudo-covariance matrix P_k^- and the state estimate $\hat{\mathbf{x}}_k^-$, are computed from

$$\hat{\mathbf{x}}_{k+1}^- = \phi\left(\hat{\mathbf{x}}_k, k\right) \tag{2}$$

$$P_{k+1}^- = \phi_{Lin} P_k \phi_{Lin}^T + \mathbf{Q}_k, \tag{3}$$

where the symmetric positive definite matrix $P_k \in R^{nxn}$ represents the updated state pseudo-covariance matrix at time instant k, the symmetric positive semi-definite matrix $Q_k \in R^{nxn}$ is the covariance matrix of the Gaussian white process noise and ϕ_{Lin} represents the state transition matrix linearized about the state estimate, i.e.

$$\phi_{Lin} = \partial\phi / \partial\mathbf{x}_k \big|_{x_k = \hat{x}_k}. \tag{4}$$

Update step: The updated state estimate $\hat{\mathbf{x}}_{k+1}$ and the updated error pseudo-covariance matrix P_{k+1} at time *k+1* are computed respectively as

$$\hat{\mathbf{x}}_{k+1} = \hat{\mathbf{x}}_{k+1}^- + \mathbf{K}_k\left[\mathbf{z}_{k+1} - h\left(\hat{x}_{k+1}^-\right)\right] \tag{5}$$

$$P_k = P_k^-\left[I - \left(\partial h/\partial\mathbf{x}_k\right)^T S_{k+1}^{-1}\left(\partial h/\partial\mathbf{x}_k\right) P_k^-\right]. \tag{6}$$

The residual pseudo-covariance matrix at time *k+1* is defined as

$$S_{k+1} = cov\left[r_{k+1}; r_{k+1}\right] = \left(\partial h/\partial\mathbf{x}_k\right) P_{k+1}^- \left(\partial h/\partial\mathbf{x}_k\right)^T + \mathbf{R}_k \tag{7}$$

where $R_k \in R^{mxm}$ is the covariance matrix of the measurement noise. The EKF gain matrix $\mathbf{K_k} \in R^{nxm}$ is defined as

$$\mathbf{K}_k = P_k\left(\partial h/\partial\mathbf{x}_k\right)^T \mathbf{R}_k^{-1}. \tag{8}$$

The residual vector at time *k+1* is

$$r_{k+1} = \mathbf{z}_{k+1} - \hat{\mathbf{z}}_{k+1}^-, \tag{9}$$

where $\hat{\mathbf{z}}_{k+1}^- = h\left(\mathbf{x}_{k+1}^-, k\right) + \mathbf{v}_{k+1}$.

3. SENSORS

This paper focuses on the design of tracking filters based on range and bearing measurements provided by an active sensor. Assuming that the target is moving underwater in the ocean, the sensor must be based on the propagation of acoustic waves, as electromagnetic waves suffer high attenuation in sea water.

A complete Ultra Short Base Line (USBL) is an active tracking system that consists of an array of hydrophones, which is usually installed underneath a ship, and a pinger or transponder mounted on the target. This system provides measurements of the distance *d* from the vehicle (target) and the respective bearing angle θ. The USBL measurements are usually obtained in polar coordinates that must be transformed to Cartesian coordinates using

$$\begin{bmatrix} d \\ \theta \end{bmatrix} = g\left(x, y\right) = \begin{bmatrix} \sqrt{x^2 + y^2} \\ tan^{-1}\left(y/x\right) \end{bmatrix}. \tag{10}$$

The inverse transformation $g^{-1}\left(d, \theta\right)$ exist everywhere except at the origin (where the distance is null)

$$\begin{bmatrix} x \\ y \end{bmatrix} = g^{-1}\left(d, \theta\right) = \begin{bmatrix} d.\cos\left(\theta\right) \\ d.\sin\left(\theta\right) \end{bmatrix} \tag{11}$$

It is considered that the sensor measurements are disturbed by noise, which can be approximated by a Gaussian distribution, see (Alves, 2004) for details.

4. TARGET TRACKING STATE MODELS

In this section, the state models considered in this work will be introduced. Both models considered will be closed related with the trajectories that an underwater vehicle executes and that can be approximated locally by circular or straight line paths (the straight line corresponds to a degenerated case of the circular path).

4.1 Circular motion state model

The model presented in this subsection is suited for vehicles performing circular paths with constant linear and angular velocities (Alves, 2004). The kinematics of the target can be described by

$$\begin{cases} \dot{\psi} = \omega \\ \dot{\mathbf{p}} = \mathbf{R}\left(\psi\right).\begin{bmatrix} \nu \\ 0 \end{bmatrix} \end{cases} \tag{12}$$

where ψ is the angle that the vehicle describes with direction of reference (e.g. the North direction), ω is the angular velocity, $\mathbf{p} = \begin{bmatrix} p_x & p_y \end{bmatrix}^T$ is the vehicle's position in R^2, $\mathbf{R}\left(\psi\right) = \begin{bmatrix} \cos\left(\psi\right) & -\sin\left(\psi\right) \\ \sin\left(\psi\right) & \cos\left(\psi\right) \end{bmatrix}$ is the rotation matrix for planar motion and ν is the vehicle's linear speed. After some algebraic manipulation (12) results in

$$\psi\left(t\right) = \psi_0 + \omega_0.\left(t - t_0\right), \tag{13}$$

$$\dot{p}_x = \nu_0 \cos\left(\psi_0 + \omega_0.\left(t - t_0\right)\right), \tag{14}$$

$$\dot{p}_y = \nu_0 \sin\left(\psi_0 + \omega_0.\left(t - t_0\right)\right), \tag{15}$$

$$\omega\left(t\right) = \omega_0, \tag{16}$$

$$\nu\left(t\right) = \nu_0. \tag{17}$$

Using (14) (15) and the rotation matrix, the position is given by

$$\mathbf{p} = \mathbf{p}_0 + \mathbf{R}\left(\psi_0\right).\left[\mathbf{I} - \mathbf{R}\left(\omega_0.\left(t - t_0\right)\right)\right].\begin{bmatrix} 0 \\ \nu_0/\omega_0 \end{bmatrix}, \tag{18}$$

that corresponds to the equation of the circumference with centre in $\mathbf{p}_0 = \begin{bmatrix} p_{x0} & p_{y0} \end{bmatrix}^T$ and radius ν_0/ω_0. We can also include in the model stochastic linear and angular accelerations that can be seen as state uncertainty allowing for the Kalman filter to take into account variations in the state variables, namely in the linear speed and angular velocity of the target. The model becomes

$$\begin{bmatrix} \psi(t) \\ p_x(t) \\ p_y(t) \\ \omega(t) \\ v(t) \end{bmatrix} = \begin{bmatrix} \psi_0 \\ p_{x0} \\ p_{y0} \\ \omega_0 \\ v_0 \end{bmatrix} + \begin{bmatrix} \omega_0 \Delta t \\ \mathbf{R}(\psi_0).\dfrac{\mathbf{I}-\mathbf{R}(\omega_0.\Delta t)}{\omega_0}.\begin{bmatrix} 0 \\ v_0 \end{bmatrix} \\ 0 \\ 0 \end{bmatrix} + \sqrt{\Delta t}\mathbf{B}\begin{bmatrix} \eta_\omega \\ \eta_v \end{bmatrix} \tag{19}$$

where Δt is the sampling period and the random variables η_ω and η_v are introduced to represent the linear speed and angular velocity derivatives, respectively. The matrix $\mathbf{B}$ is defined by $B=\begin{bmatrix} 0 & 0 & 0 & 1 & 0 \\ 0 & 0 & 0 & 0 & 1 \end{bmatrix}^T$. The covariance of the Gaussian white process noise is given by

$$\mathbf{Q}_k = blkdiag\left(\mathbf{0}_{3\times 3}, \Delta t\begin{bmatrix} \sigma_\omega^2 & 0 \\ 0 & \sigma_v^2 \end{bmatrix}\right), \tag{20}$$

where *blkdiag* represents a block diagonal matrix, σ_ω^2 and σ_v^2 are the variance of the random variables η_ω and η_v, respectively.

Circular motion state model with known angular velocity.

In the case where the angular velocity is known *a priori*, for instance in pre-programmed missions to be carried out by Autonomous Underwater Vehicles (AUVs), this variable is no longer required to be estimated. Then, the model described in (19) can be simplified to give

$$\begin{bmatrix} \psi(t) \\ p_x(t) \\ p_y(t) \\ v(t) \end{bmatrix} = \begin{bmatrix} \psi_0 \\ p_{x0} \\ p_{y0} \\ v_0 \end{bmatrix} + \begin{bmatrix} \omega_0 \Delta t \\ \mathbf{R}(\psi_0).\dfrac{\mathbf{I}-\mathbf{R}(\omega_0.\Delta t)}{\omega_0}.\begin{bmatrix} 0 \\ v_0 \end{bmatrix} \\ 0 \end{bmatrix} + \eta_v.\sqrt{\Delta t}\begin{bmatrix} 0 \\ 0 \\ 0 \\ 1 \end{bmatrix}. \tag{21}$$

The covariance is defined as in (20) deleting the rows and columns that correspond to the angular velocity.

4.2 Constant turn model with known turn rate

This dynamic model is derived from the standard curvilinear-motion model kinematics of a target moving in the horizontal plane (Rong and Jilkov, 2003)

$$\begin{cases} \dot{\psi} = a_n(t)/v(t) \\ \dot{p}_x = v(t)\cos\psi(t), \\ \dot{p}_y = v(t)\sin\psi(t) \\ \dot{v}(t) = a_t(t) \end{cases} \tag{22}$$

where p_x and p_y are the target linear position in the inertial frame, v is the vehicle's linear speed, ψ is the angle that the vehicle does in relation to a reference direction and a_t and a_n are the target tangential and normal accelerations in the horizontal plane. This kinematic model is fairly general as it takes into account along and cross accelerations. A particular case of interest for the envisaged application is a constant speed and constant turn rate motion. The normal and tangential acceleration are then constant and zero $(a_n = a_{n0} = \text{cte},\ a_n \neq 0)$, respectively. Then, the first equation of (22) can be simplified to

$$\dot{\psi} = \omega, \tag{23}$$

where ω is the vehicle's angular velocity. It follows from (22) and (23) that such circular motion can be described by

$$\dot{\mathbf{x}} = \begin{bmatrix} \dot{x}(t) & -\omega\dot{y}(t) & \dot{y}(t) & \omega\dot{x}(t) \end{bmatrix}^T + \mathbf{G}\mathbf{w}(t) \tag{24}$$

where $\mathbf{x} = \begin{bmatrix} p_x & \dot{p}_x & p_y & \dot{p}_y \end{bmatrix}^T$ and $\mathbf{Gw}(t)$ are the stochastic accelerations that represent uncertainty in respective state variables and allow for variations in the state, defined by

$$\mathbf{G} = \begin{bmatrix} 0 & 1 & 0 & 0 \\ 0 & 0 & 0 & 1 \end{bmatrix}^T \quad \mathbf{w}(t) = \begin{bmatrix} w_x & w_y \end{bmatrix}^T \tag{25}$$

The discrete-time equivalent can then be written in the form

$$\mathbf{x}_{k+1} = \phi_k \mathbf{x}_k + \mathbf{w}_k, \tag{26}$$

where

$$\phi_k = e^{\mathbf{F}\Delta t} = \begin{bmatrix} 1 & \dfrac{\sin\omega\Delta t}{\omega} & 0 & -\dfrac{1-\cos\omega\Delta t}{\omega} \\ 0 & \cos\omega\Delta t & 0 & -\sin\omega\Delta t \\ 0 & \dfrac{1-\cos\omega\Delta t}{\omega} & 1 & \dfrac{\sin\omega\Delta t}{\omega} \\ 0 & \sin\omega\Delta t & 0 & \cos\omega\Delta t \end{bmatrix}, \tag{27}$$

$$\mathbf{w}_k = \begin{bmatrix} \dfrac{\sin\omega\Delta t}{\omega} & -\dfrac{1-\cos\omega\Delta t}{\omega} \\ \cos\omega\Delta t & -\sin\omega\Delta t \\ \dfrac{1-\cos\omega\Delta t}{\omega} & \dfrac{\sin\omega\Delta t}{\omega} \\ \sin\omega\Delta t & \cos\omega\Delta t \end{bmatrix}\begin{bmatrix} \eta_x \\ \eta_y \end{bmatrix}, \tag{28}$$

with η_x and η_y random variables that represent unknown accelerations. The covariance matrix can be computed from (Brown and Hwang, 1997)

$$\mathbf{Q}_k = \int_{t_k}^{t_{k+1}}\int_{t_k}^{t_{k+1}} \phi(t_{k+1},\xi)\mathbf{G}(\xi)E\left[\mathbf{w}(\xi)\mathbf{w}^T(\tau)\right].\mathbf{G}^T(\tau)\phi^T(t_{k+1},\tau)\,d\xi d\tau \tag{29}$$

The resulting expression is omitted due to complexity.

4.3 Evaluation of the Target Tracking State Models

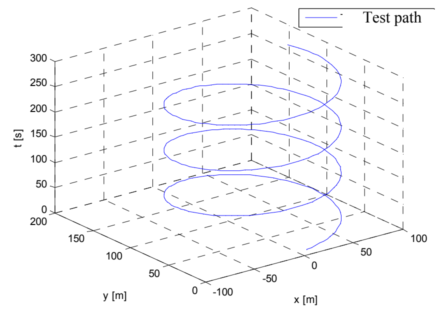

Fig. 1. Test path used to perform the models simulation.

Both models were simulated considering that the vehicle was describing a circular path as depicted in Fig. 1. Monte Carlo simulations were performed to assess the performance of the estimation algorithm presented in previous section. The mean squared error of the linear position estimates as function of the distance and angle sensors noise standard deviation are summarized in Table 1.

Table 1 Mean squared error obtained for several noise variance for both state models

		Circular motion state model		Constant model with known Turn Rate	
Noise Variance		Mean squared error		Mean squared error	
distance [m^2]	angle [$(°)^2$]	px error	py error	px error	py error
$0,01^2$	$0,01^2$	5,275E-03	4,102E-03	8,059E-02	6,366E-02
$0,05^2$	$0,05^2$	1,518E-02	1,345E-02	1,865E-01	1,420E-01
$0,1^2$	1^2	9,813E-02	6,894E-02	4,033E-01	3,196E-01
1^2	2^2	2,242E-01	1,727E-01	6,084E-01	5,563E-01
3^2	2^2	3,621E-01	4,414E-01	6,643E-01	6,233E-01
4^2	3^2	4,929E-01	5,273E-01	7,388E-01	6,774E-01
4^2	4^2	5,665E-01	5,280E-01	7,921E-01	7,049E-01
5^2	4^2	6,704E-01	6,435E-01	8,098E-01	7,275E-01
5^2	5^2	7,595E-01	6,721E-01	8,761E-01	7,656E-01
5^2	6^2	9,977E-01	8,526E-01	9,458E-01	8,065E-01
6^2	6^2	9,320E-01	8,383E-01	9,673E-01	8,337E-01

From the results presented in Table 1 it can be concluded that the circular motion state model presents better performance than that obtained with the constant turn rate model for all noise conditions tested. The performance of the estimation algorithms degrades gracefully with noise. It is interesting to notice that the mean squared error of both estimation algorithms get closer for high noise standard deviations.

5. NONLINEAR ESTIMATION PERFORMANCE

The problem of estimating the state variables for a discrete time nonlinear dynamic system, with discrete nonlinear observations corrupted by additive Gaussian white noise, arises in many applications. Since the optimality of the estimation algorithms developed is not guaranteed by the design procedure, an important step is the analysis of the lower bound for the estimation problem at hand. Then the comparison of the performance obtained for a given algorithm to the lower bound determines if a more effective algorithm design is required. A powerful result to determinate the best performance attainable in an estimation problem is the so-called Cramér-Rao lower bound (Kay, 1993). Defining P as the estimation error covariance matrix corresponding to any unbiased estimator, then this inequality can be stated as

$$\mathbf{P} \geq \mathbf{P}^{*} = J^{-1} \qquad (30)$$

where J is the *Fisher* information matrix, P^{*} is the estimation lower bound, and $\mathbf{A} \geq \mathbf{B}$ means that $\mathbf{A}-\mathbf{B}$ is non defined negative.

5.1 Cramér-Rao Lower Bound

Let x be an unknown deterministic parameter and z the vector of observations, corrupted by noise with known probability density function (pdf) $p(\mathbf{z};\mathrm{x})$. If the pdf satisfies the regularity condition (Kay, 1993)

$$E\left[\frac{\partial ln\, p(\mathbf{z};\mathrm{x})}{\partial \mathrm{x}}\right] = 0,\ \forall \mathrm{x} \qquad (31)$$

the variance of any unbiased estimator satisfies

$$var(\hat{\mathrm{x}}) \geq \frac{1}{-E\left[\dfrac{\partial^2 ln\, p(\mathbf{z};\mathrm{x})}{\partial \mathrm{x}^2}\right]} \qquad (32)$$

where the denominator is the well known Fisher information matrix

$$J(\mathrm{x}) = -E\left[\frac{\partial^2 ln\, p(\mathbf{z};\mathrm{x})}{\partial \mathrm{x}^2}\right] \qquad (33)$$

and the lower bound on the variance of any estimator is given by

$$var(\hat{\mathrm{x}}) = J(\mathrm{x})^{-1}. \qquad (34)$$

For the specific case studied here a deeper analysis will be performed based in Taylor's method. Assuming that the system is written in the form presented in (1) and is not corrupted with any process noise $\mathbf{w}_k = \mathbf{0}$, the pdf $p(\mathbf{Z}_k \mid \mathbf{X}_k)$ can be defined as (Taylor, 1979; Kerr, 1989; Level, 2006)

$$p(\mathbf{Z}_k \mid \mathbf{X}_k) = \frac{1}{(2\pi)^{n/2}|\mathbf{S}_0|^{1/2}} exp\left\{-1/2(\mathbf{x}_0-\hat{\mathbf{x}}_0)^T \mathbf{S}_0^{-1}(\mathbf{x}_0-\hat{\mathbf{x}}_0)\right\}\cdot$$
$$\prod_{k=1}^{K}\frac{1}{(2\pi)^{m/2}|\mathbf{R}_k|^{1/2}} exp\left\{-1/2(\mathbf{z}_k-h(\mathbf{x}_k))^T \mathbf{R}_k^{-1}(\mathbf{z}_k-h(\mathbf{x}_k))\right\} \qquad (35)$$

where $\hat{\mathbf{x}}_0 \sim N(\mathbf{x}_0,\mathbf{S}_0)$, $\mathbf{Z}_k = \{\mathbf{z}_0,\mathbf{z}_1,\ldots,\mathbf{z}_K\}$ and $\mathbf{X}_k = \{\mathbf{x}_0,\mathbf{x}_1,\ldots,\mathbf{x}_K\}$. Taking the logarithm of (35) and then the expectation of the second partial in accordance with (33), we obtain

$$J_k = \left(\frac{\partial \mathbf{x}_0}{\partial \mathbf{x}_K}\right)^T \mathbf{S}_0^{-1}\left(\frac{\partial \mathbf{x}_0}{\partial \mathbf{x}_K}\right) + \sum_{k=1}^{K}\left(\frac{\partial h_k}{\partial \mathbf{x}_K}\right)^T \mathbf{R}_k^{-1}\left(\frac{\partial h_k}{\partial \mathbf{x}_K}\right). \qquad (36)$$

Defining

$$\mathbf{H}_k = \left.\frac{\partial h(\mathbf{x}_k,\mathrm{k})}{\partial \mathbf{x}_k}\right|_{\mathbf{x}_k}, \qquad (37)$$

and applying the chain rule of partial differentiation to equation (36), yields

$$J_k = \left(\frac{\partial \mathbf{x}_0}{\partial \mathbf{x}_K}\right)^T \mathbf{S}_0^{-1}\left(\frac{\partial \mathbf{x}_0}{\partial \mathbf{x}_K}\right) + \sum_{k=1}^{K}\left(\frac{\partial \mathbf{x}_k}{\partial \mathbf{x}_K}\right)^T \mathbf{H}_k^T \mathbf{R}_k^{-1} \mathbf{H}_k \left(\frac{\partial \mathbf{x}_k}{\partial \mathbf{x}_K}\right).$$

Defining

$$\frac{\partial \mathbf{x}_k}{\partial \mathbf{x}_K} = \frac{\partial \boldsymbol{\phi}_k}{\partial \mathbf{x}}, \qquad (39)$$

equation (38) can be written in a recursive form in terms of P^* as

$$J_k = \left(P_k^*\right)^{-1} = \left[\left(\frac{\partial \boldsymbol{\phi}_k}{\partial \mathbf{x}}\bigg|_{\mathbf{x}_k}\right)\mathbf{P}_{k-1}^*\left(\frac{\partial \boldsymbol{\phi}_k}{\partial \mathbf{x}}\bigg|_{\mathbf{x}_k}\right)^T\right]^{-1} + \mathbf{H}_k^T \mathbf{R}_k^{-1} \mathbf{H}_k . \qquad (40)$$

5.2 Posterior Cramér-Rao Bound

The Posterior Cramér-Rao Bound (PCRB) provides a mean-square error lower bound for the discrete time nonlinear filtering problem. This lower bound is applicable to multidimensional nonlinear dynamical systems, corrupted by disturbances not necessarily Gaussian, and is more general than other approaches described in the literature (Tichavský, Muravchik, Nehorai, 1998). This approach can also deal with process noise, so the Fisher matrix is defined as

$$J = -E\left[\nabla_{\mathbf{x}}\left\{\left(\nabla_{\mathbf{x}}\, ln\, p\left(\mathbf{X}_k, \mathbf{Z}_k\right)\right)^T\right\}\right], \qquad (41)$$

where $\nabla_{\mathbf{x}} = \left[\frac{\partial}{\partial x_1}, \ldots, \frac{\partial}{\partial x_k}\right]$ is the Jacobian. In this case both $\mathbf{Z}_k$ and $\mathbf{X}_k$ are random variables, instead of $\mathbf{X}_k$ being deterministic as for the Cramér-Rao Lower Bound (CRLB). So, the pdf is now defined as

$$p\left(\mathbf{X}_k, \mathbf{Z}_k\right) = p\left(\mathbf{x}_0\right)\prod_{i=1}^{k} p\left(\mathbf{z}_i \mid \mathbf{x}_i\right)\prod_{j=1}^{k} p\left(\mathbf{x}_j \mid \mathbf{x}_{j-1}\right). \qquad (42)$$

In (Tichavský, Muravchik, Nehorai, 1998) it is shown that the *Fisher* matrix in recursive form is

$$J_{k+1} = D_k^{22} - D_k^{21}\left(J_k + D_k^{11}\right)^{-1} D_k^{12}, \qquad (43)$$

where, in the general case,

$$D_k^{11} = E\left[-\nabla_{\mathbf{x}_k}\nabla_{\mathbf{x}_k}^T\, ln\, p\left(\mathbf{x}_{k+1} \mid \mathbf{x}_k\right)\right], \qquad (44)$$

$$D_k^{12} = E\left[-\nabla_{\mathbf{x}_k}\nabla_{\mathbf{x}_{k+1}}^T\, ln\, p\left(\mathbf{x}_{k+1} \mid \mathbf{x}_k\right)\right] = \left[D_k^{21}\right]^T, \qquad (45)$$

$$\begin{aligned} D_k^{22} &= E\left[-\nabla_{\mathbf{x}_{k+1}}\nabla_{\mathbf{x}_{k+1}}^T\, ln\, p\left(\mathbf{x}_{k+1} \mid \mathbf{x}_k\right)\right] \\ &\quad + E\left[-\nabla_{\mathbf{x}_{k+1}}\nabla_{\mathbf{x}_{k+1}}^T\, ln\, p\left(\mathbf{z}_{k+1} \mid \mathbf{x}_{k+1}\right)\right]. \end{aligned} \qquad (46)$$

Simplifying under the assumption of white Gaussian noise, equations given by (44), (45) and (46) result in

$$D_k^{11} = \left[\nabla_{\mathbf{x}_k}\phi_k\left(\mathbf{x}_k\right)\right]^T \mathbf{Q}_k^{-1}\left[\nabla_{\mathbf{x}_k}\phi_k\left(\mathbf{x}_k\right)\right], \qquad (47)$$

$$D_k^{12} = -\left[\nabla_{\mathbf{x}_k}\phi_k\left(\mathbf{x}_k\right)\right]^T \mathbf{Q}_k^{-1} = \left[D_k^{21}\right]^T, \qquad (48)$$

$$D_k^{22} = \mathbf{Q}_k^{-1} + \left[\nabla_{\mathbf{x}_{k+1}} h\left(\mathbf{x}_{k+1}\right)\right]^T \mathbf{R}_k^{-1}\left[\nabla_{\mathbf{x}_{k+1}} h\left(\mathbf{x}_{k+1}\right)\right]. \qquad (49)$$

The *Fisher* matrix previously introduced in (43) is simplified to

$$\begin{aligned} J_{k+1} = &\left(\left[\nabla_{\mathbf{x}_k}\phi_k\left(\mathbf{x}_k\right)\right] J_k^{-1}\left[\nabla_{\mathbf{x}_k}\phi_k\left(\mathbf{x}_k\right)\right]^T + \mathbf{Q}_k\right)^{-1} + \\ &+ \left[\nabla_{\mathbf{x}_{k+1}} h\left(\mathbf{x}_{k+1}\right)\right]^T \mathbf{R}_{k+1}^{-1}\left[\nabla_{\mathbf{x}_{k+1}} h\left(\mathbf{x}_{k+1}\right)\right] \end{aligned} \qquad (50)$$

Comparing (50) to (40), it is apparent that these two equations are identical, which leads to a interesting conclusion(38)Taylor's method for computing the CRLB can be easily adapted to compute an approximate PCRB by simply including the process noise covariance. It is important to notice that the linearization of the system dynamics in (37), (40) and (50) should be obtained about the nominal path (an equilibrium path for the dynamics) considered in simulation.

6. MODELS PERFORMANCE – RESULTS AND DISCUSSION

In order to analyze the performance of both estimation algorithms the Cramer-Rao and Posterior Cramer-Rao lower bounds were computed for the problem at hand. First a CRLB analysis was carried out, where uncorrupted process models were considered. The results are summarized and in Fig. 2. and Fig. 3.

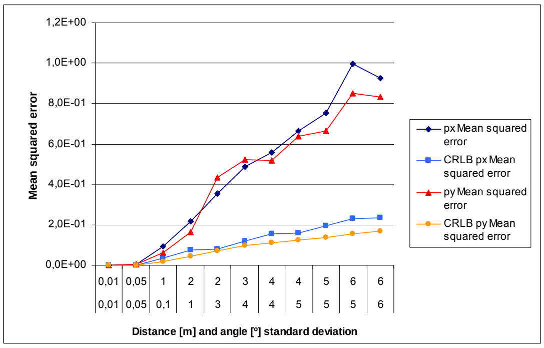

Fig. 2. Position estimation performance and CRLB results using the circular motion state model.

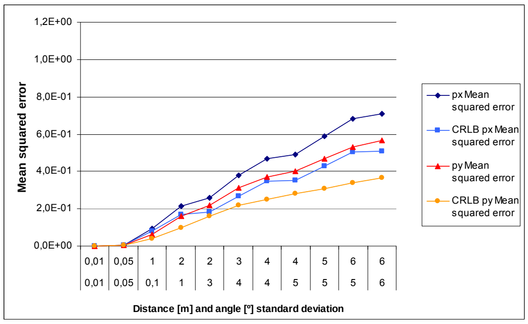

Fig. 3. Position estimation performance and CRLB results using the constant model with known turn rate.

From the results depicted in Fig. 2. and Fig. 3., it can be concluded that the constant model with known turn rate has better performance than the circular motion state model. Notice that the estimation performance is quite similar for both models for low noise variances. As the noise variance increases the estimation performance degrades but the constant model with known turn rate becomes more accurate than the circular motion state model.

Next a Posterior Cramer-Rao lower bound analysis was performed. The results are summarized in Fig. 4. and Fig. 5.

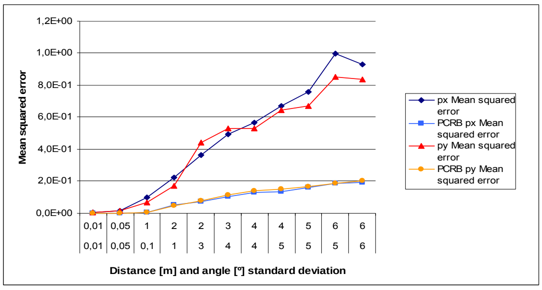

Fig. 4. Position estimation performance and PCRB results using the circular motion state model.

In these figures the circular motion state model has shown better performance than the constant model with known turn rate, almost for all noise variances considered in the simulation. However these results, when compared with the corresponding posterior lower bounds, allow one to conclude that there might be other estimation techniques that can provide better estimates, thus near the PCRLB.

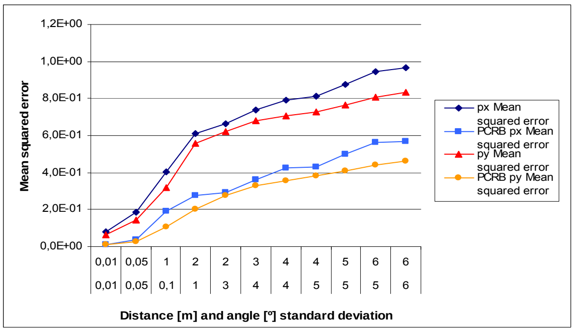

Fig. 5. Position estimation performance and PCRB results using the constant model with known turn rate.

From the results obtained, it is also possible to conclude that the performance of the algorithm, although degraded for higher noise variances, becomes similar.

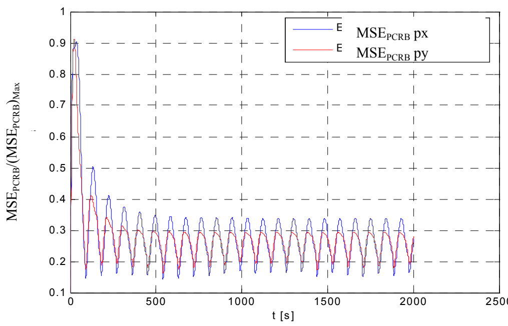

Fig. 6. Mean squared error (MSE) evolution for the constant model with known turn rate using the optimal estimator derived with PCRB theory.

Notice the periodic evolution of the mean square error in the optimal situation derived with PCRB theory, as depicted in Fig. 6. This evolution reveals the impact of the geometry of mission on the estimation problem performance, i.e. due to the circular motion performed by the vehicle. The estimated on the coordinate x has higher uncertainty when the vehicle is far from the sensor in the coordinate y. Similarly, for the coordinate x higher uncertainty in the coordinate x occurs when the vehicle is far from the sensor in coordinate y. This fact is justified due to the noise that corrupts the bearing angle that, for higher distances, results on larger uncertainty in the estimation of the vehicle position.

7. CONCLUSIONS

In this paper two different dynamic models for target tracking were presented. The performance of the Extended Kalman filters for the estimation of the unknown quantities, in both models, was studied. The results obtained show that the proposed algorithms can be further improved, due to the fact that the mean squared estimate errors are relatively far from the optimal solution.

Comparatively, the circular motion state model has better performance than the constant model with known turn rate in the case where it was considered process noise in the system. In the case with no process noise, the constant model with known turn rate had better performance. Although it was interesting to see that the estimation performance of both models, in both situations referred previously, become closer as the noise variance increases. The performance of both algorithms is improved for lower signal to noise ratios. The analyses performed in this work lead us to the conclusion that the uncertainty affecting the bearing angle had great influence in the performance of the algorithms.

REFERENCES

Alcocer, A., P. Oliveira P. and A. Pascoal. (2007)

Study and Implementation of an EKF GIB-based Underwater Positioning System," IFAC Journal of Control Engineering Practice, vol 15, pp.689-701.

Alves, P. M. (2004)

Seguimento e predição da trajectória de alvos móveis em duas dimensões. Tese de Mestrado. UTL, IST, Lisboa.

Brown, R. G. and P.Y.C. Hwang. (1997)

Introduction to Random Signals and Applied Kalman Filtering. John Wiley & Sons, third edition.

Gelb, A. (1974).

Applied Optimal Estimation.MIT Press.

Kay, Steven M. (1993)

Fundamentals of Statistical Signal Processing: Estimating Theory. Prentice Hall.

Kerr, Thomas H. (1989)

Status of CR-Like Lower Bounds for Nonlinear Filtering. In: *IEEE Trans. on Aerospace and Electronic Systems*. **vol. 25**, pp 590-597.

Level, William F. (2006)

Approximate Cramér-Rao Bound for Multiple Target Tracking. PhD Thesis, Georgia Institute of Technology.

Rong, X. Li and Vesselin P. Jilkov. (2003)

Survey Maneuvering Target Tracking. In: *IEEE Trans. on Aerospace and Electronic Systems*. **vol. 39**, pp 1333-1364.

Rugh, Wilson J. (1996)

Linear System Theory. Prentice-Hall, second edition. USA.

Taylor, James H. (1979)

The Cramér-Rao Estimation Error Lower Bound Computation for Deterministic Nonlinear Systems. In: *IEEE Trans. on Automatic Control*. **vol. AC-24**, pp 343-344.

Tichavský, Petr, Carlos H. Muravchik and Arye Nehorai. (1998)

Posterior Cramér-Rao Bounds for Discrete-Time Nonlinear Filtering. In: *IEEE Trans. on Signal Processing*. **vol. 46**, pp 1386-1396.